UDC 539.23:620.18:620.17

A. A. Onoprienko*, V. I. Ivashchenko, I. I. Timofeeva, A. K. Sinelnitchenko, O. A. Butenko (Kiev)
**onopr@ipms.kiev.ua*

Characterization of Ti–B–C–N films deposited by dc magnetron sputtering of bicomponent Ti/B_4C target

Quaternary Ti–B–C–N films have been deposited onto Si (100) substrates by dc magnetron sputtering of bi-component Ti/B_4C target in an Ar/N_2 gas mixture with different amounts of nitrogen in the mixture (from 0 to 50%). The X-ray diffraction, X-ray photoelectron spectroscopy, indentation, and scratch tests have been employed to characterize the films. The films have been found to have the nanocomposite structure composed of Ti/TiB nanocrystallites (nc) solely when sputtered in argon or of nanocrystallite nc-TiN/nc-TiB_x/nc-TiO_x phases embedded into an amorphous a-C/a-CN/a-BN/a-BC matrix when nitrogen is added to the gas mixture. The latter structure is specific of all the films deposited with nitrogen irrespective of the nitrogen amount in the gas mixture. It has been found that the Knoop hardness of films first increased with added nitrogen reaching maximum value of 33 GPa at 25% N_2 in the gas mixture, and then decreased. The friction coefficient of films changed little with the added nitrogen, while with 25% N_2 exhibited the lowest value. The Ti–B–C–N films showed increased adhesion strength on silicon compared with Ti–B–C coatings.

Keywords*: magnetron sputtering, nanocomposite, structure, mechanical properties.*

INTRODUCTION

Nanostructured multicomponent and multiphase thin films or coatings are now extensively studied in the development of new engineering materials [1–3]. These materials are formed by a mixture of components, which typically consist of nanometer sized crystals embedded into an amorphous or nanocrystalline matrix. Among a variety of these materials the Ti transition metal nitrides and carbides (such as TiN and TiC) of binary and Ti–C–N and Ti–B–N ternary systems are attractive materials because of their high hardness, high melting point, chemical inertness, good wear and corrosion resistance [4–7]. For these reasons, they have been used for hard wear-resistant coatings in machining industry, diffusion barriers in microelectronics, and electrodes in semiconductor devices. The demand for advanced coatings with further improved mechanical, corrosion, and tribological properties has recently led to more complex coatings, in particular of Ti–B–C–N system [7–12].

Nanocomposite coatings of the Ti–B–C–N system can be obtained by a variety of methods, such as dc or rf reactive (in the mixture of argon and nitrogen gases) magnetron sputtering of TiB_2/TiC composite target [7], Ti/B_4C compound target [8], separate C, Ti, and TiB_2 targets [9], separate C, Ti, and B_4C targets [10], single Ti and TiB_2 targets (in this case sputtering is carried out in the mixture of argon,

nitrogen, and acetylene gases) [11]. The methods of cathodic arc plasma evaporation [9] and CVD (in which various precursors are used) [13–15] have also been applied for deposition of coatings of the Ti–B–C–N system.

In this work we propose an alternative rather simple approach for deposition of hard Ti–B–C–N films, based on the dc magnetron sputtering in an Ar/N_2 gas mixture of targets composed of elements that form the film. This method allows controlling the content of constituting elements through the variation of amount of them in the target. The Ti–B–C–N films were synthesized on silicon substrates by dc magnetron sputtering of single bi-component target. The X-ray diffraction (XRD), X-ray photoelectron spectroscopy (XPS), indentation and scratch tests were used to study the microstructure, phase composition, binding state and mechanical properties of Ti–B–C–N films.

EXPERIMENTAL

Multicomponent film deposition

The Ti–B–C–N films were deposited onto Si (100) substrates by dc magnetron sputtering of bi-component Ti/B_4C target in an Ar/N_2 gas mixture. The base component of target was titanium as a disk (60 mm in diameter and 3 mm in thickness), in the sputtering zone of which platelet chips of boron carbide (B_4C) were attached. The chips had the size of about 4×4 mm. By this approach the composition of deposited films could be varied through the ratio between surface areas of titanium and boron carbide in the target. In our experiments the amount of B_4C chips was unchanged, and the Ti to B_4C surface area ratio was about 10:1.

The dc magnetron operated at sputtering power of 100 W. The distance between target and substrates was 50 mm. The substrates were preliminarily chemically etched in a 10 % aqueous solution of hydrofluoric (HF) acid in order to remove the oxidized layer from the substrate surface, and then ultrasonically treated in a bath of ethanol and acetone mix (50:50) and dried. The working chamber was pumped to residual pressure of $2.7 \cdot 10^{-3}$ Pa. The substrate surface was pre-sputtered by Ar ions at a negative bias voltage of 600 V for 15 min prior to a film deposition. For the film deposition the chamber was first filled with argon to a pressure of 0.4 Pa, and then the nitrogen was added to gas mixture in various amounts, so that the component ratios in Ar/N_2 mixture were 75% Ar + 25% N_2, 60% Ar + 40% N_2, and 50% Ar + 50% N_2. For comparison we also deposited the film in 100% Ar plasma. The bias voltage was not applied to the substrates, but were under floating potential during the deposition. The substrates were not preheated, however, during the deposition the substrate temperature reached a value of about 200°C due to the plasma heating. A total of four films have been deposited of 0.7–2.0 μm in thickness differing in composition.

Characterization of Ti–B–C–N films

The film thickness was determined using a Micron-Alpha (Ukraine) optical profilometer with an accuracy of ±5 nm via a step formed in the film due to masking of the substrate surface before the film deposition. The crystal structure of as-deposited Ti–B–C–N films was examined by XRD (DRON-3 diffractometer) in Θ–2Θ configuration using Cu$K\alpha$ radiation. The crystallite sizes of the films were evaluated from the broadening of peaks in X-ray diffraction spectra using the Scherrer formula. The chemical bonding status of the films was observed by XPS (UHV-Analysis-System ES-2401, Russia) using Mg$K\alpha$ radiation (E = 1253.6 eV). The base pressure in the sublimation chamber was less than 10^{-8} mbar. Prior to

XPS analysis, argon etching of film surface was performed at incident energy of 1.5 keV and current density of 11 μA/cm^2. The XPS spectra were accounted at constant pass energy of 20 eV. The Au $4f_{7/2}$ and Cu $2p_{3/2}$ peaks with binding energy at 84.0±0.05 eV and 932.66±0.05 eV, respectively, were used as references.

Mechanical properties

The hardness of films was determined through indentation tests by a Micromet 2103 (Bluehler Ltd., Japan–Germany) microhardness tester at a load of 100 mN. This load was chosen in order to provide a prominent plastic deformation of film while avoiding the influence of the substrate material. Six indentations were made on each sample. The scratch tests were carried out by using the Micron-Gamma tester equipped with a Vickers pyramidal tip having a rounded radius of about 1.0 μm. The tests have been carried out at the loading rate 0.01 N/s over 158–230 μm distance. From these tests the friction coefficient and the critical load of delamination were evaluated. The tests were performed at room temperature and about 50% humidity.

RESULTS AND DISCUSSION

Microstructure and chemical composition

The phase composition of Ti–B–C–N films was examined by XRD. Figure 1 shows the X-ray diffraction patterns of films deposited at various nitrogen contents of sputtering gas mixture. The XRD pattern for the film deposited in 100% Ar plasma exhibited only one narrow intense peak at 2Θ = 38.2° corresponding to Ti (101) and TiB (111) crystalline phases [16]. So, that film is supposed to contain both Ti and TiB phases. The average crystallite size estimated by the Scherrer formula is about 17 nm. Therefore, these phases can be considered as nanocrystalline (nc) ones.

With addition of nitrogen in the amount of 25% to the gas mixture the Ti/TiB peak at 2Θ = 38.2° disappeared in diffraction pattern, and less intensive and broadened peaks centered at 2Θ ≈ 36°, 2Θ ≈ 42°, and 2Θ ≈ 61.8° appeared. The first two peaks span from about 2Θ = 35.2° to 2Θ = 36.9° and from about 2Θ = 41.3° to 2Θ = 43.2°, respectively. The broadening of those peaks can be caused by two factors, namely, the multi-component nature of the film and small size of the crystallites. The average crystallite size estimated by Scherrer formula for that film was about 3.5 nm. So, it is evident that addition of nitrogen to the sputtering gas mixture resulted in a noticeable grain refinement. Based on the reference data [16], the above peaks can be attributed to the following crystalline phases: TiN_x, TiB_x, TiC, TiO_x.

With increasing nitrogen amount in the gas mixture up to 40% the peak centered at 2Θ ≈ 36° virtually disappeared; whereas the peaks centered at 2Θ ≈ 42° and 2Θ ≈ 61.8° became sharper. The average crystallite size estimated by Scherrer formula with peak at 2Θ ≈ 42° was about 3.5 nm just as in the film deposited with 25% N_2 in the gas mixture. The analysis of the above peaks with the reference data [16] showed that the film deposited with 40% N_2 contained the same phases as the film deposited with 25% N_2.

An increase of the nitrogen amount in the gas mixture up to 50% resulted in further changes in a diffraction pattern. In particular, the intensity of peaks centered at 2Θ ≈ 42° and 2Θ ≈ 61.8° decreased noticeably, whereas the peak at 2Θ ≈ 43.4° became more prominent. The latter peak corresponds to TiO phase (2Θ ≈ 43.37° [16]). And again, analysis of peaks by reference data [16] showed that this

film contained the same phases as the films deposited with 25% and 40% N_2 in the gas mixture.

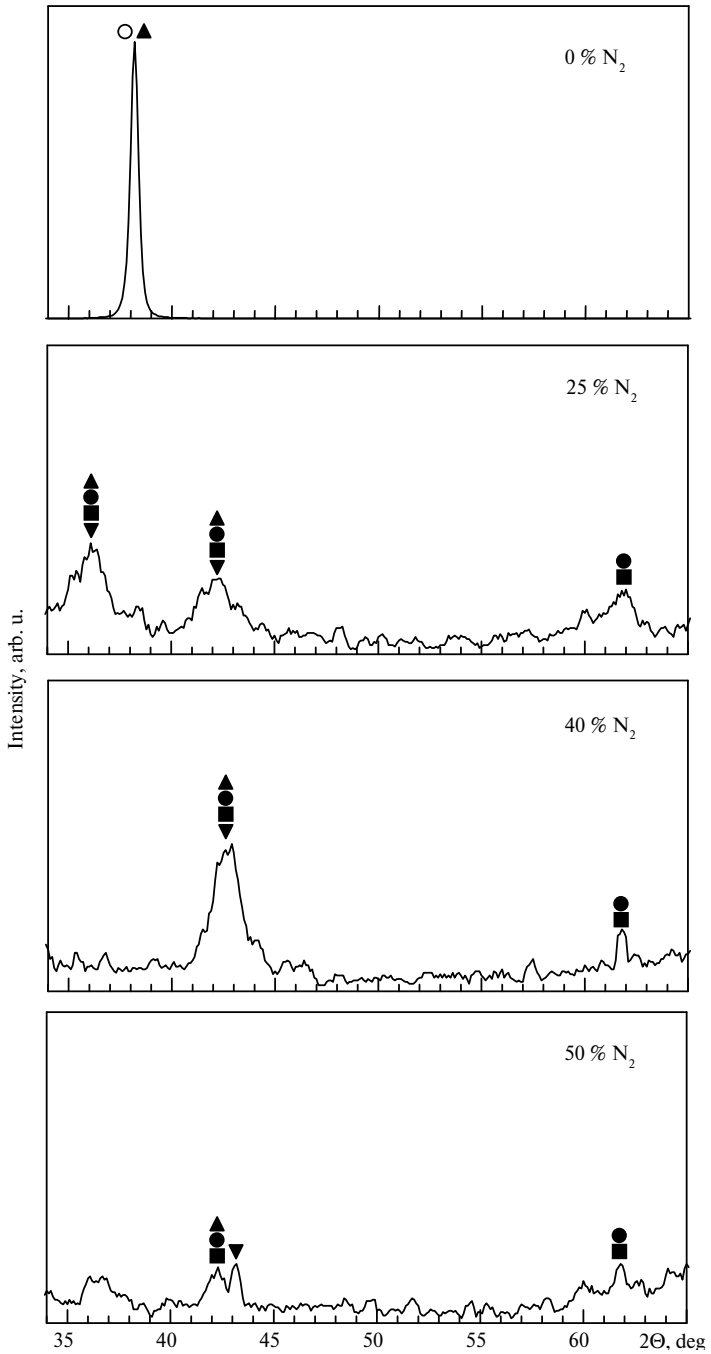

Fig. 1. XRD spectra of Ti–B–C–N films deposited with different amounts of nitrogen in Ar/N gas mixture; Ti (○), TiB (▲), TiO (▼), TiN (■) and TiC (●) phases are indicated.

To get information about the bonding state of deposited Ti–B–C–N films, the XPS analysis has been carried out using peak assignments from the published data [10, 17–21]. The XPS spectra for all the deposited Ti–B–C–N films were similar

and typical Ti2p, N1s, C1s and O1s core-level spectra and their fittings are shown in Fig. 2.

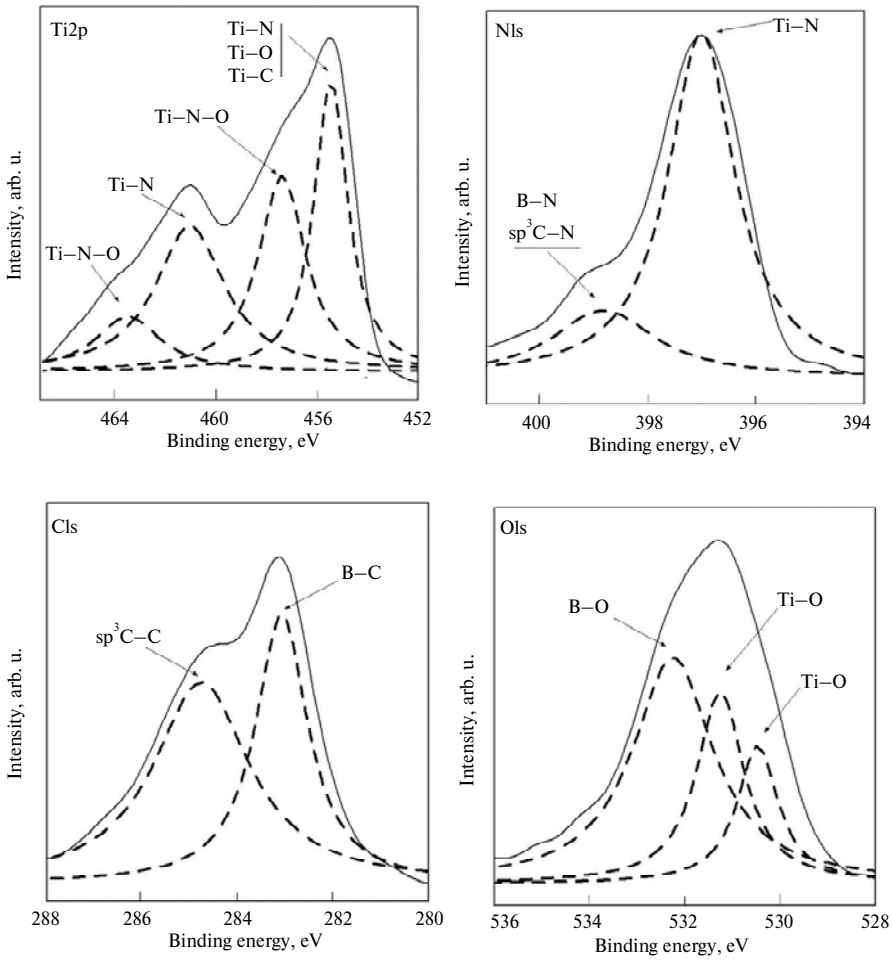

Fig. 2. Typical XPS spectra of the Ti2p (*a*), N1s (*b*), C1s (*c*) and O1s (*d*) regions of the Ti–B–C–N films under study.

The deconvoluted Ti2p spectrum (see Fig. 2, *a*) clearly indicates different chemical environments of titanium atoms. In particular, the spectrum contains $Ti2p_{3/2}$ features at 455.5 eV and $Ti2p_{1/2}$ at 461.0 eV, which can be assigned to Ti–N bonds in TiN [10, 17], and $Ti2p_{3/2}$ features at 457.4 eV and $Ti2p_{1/2}$ at 463.5 eV, which can be assigned to Ti–N–O bonds [10, 18]. The feature at 455.5 eV can also be associated with TiO and TiC compounds (455.3 eV [21]).

The N1s spectrum shown in Fig. 2, *b* is typical to that for TiN [17] and consists of two peaks centered at 397.0 eV and 398.8 eV. These peaks arise from Ti–N [18] and sp^3C–N [20], respectively. The feature at 398.8 eV can also indicate the presence of B–N bonds [21]. The tail to higher binding energies can be caused by N–O bonding [17]. The C1s spectrum (see Fig. 2, *c*) can be fitted by two peaks centered at 283.1 eV and 284.8 eV and associated with B–C and sp^2C–C bonds, respectively [10, 17]. Finally, the deconvoluted O1s spectrum (see Fig. 2, *d*)

contains three features, which can be attributed to Ti–O (530.5 eV and 531.2 eV) and B–O (532.2 eV) bonds [21].

As the XRD pattern shows, the film deposited in merely argon plasma most likely contained pure Ti and TiB_x crystalline phases. Addition of nitrogen to a gas mixture resulted in a change of the film structure. Based on the XRD pattern and Ti2p and N1s spectra, we can assume the nanocrystalline phase TiN with (111) and (200) preferential orientations to be dominant in the structure of Ti–B–C–N film deposited from a gas mixture with 25% N_2. With further increase of the nitrogen amount in the gas mixture up to 40%, the TiN phase with only (200) preferential orientation formed in the film structure. However, taking into account the broadening of XRD peaks and the C1s and O1s spectra it is reasonable to suggest that boron, carbon, and oxygen atoms replaced some nitrogen atoms in TiN grains, thus resulting in multicomponent crystalline phase $Ti(N,B,C,O)_x$ in the film structure. The N1s and C1s spectra revealed the C–N, B–N, B–C, and C–C bonds in the Ti–B–C–N films. But XRD pattern didn't show any crystalline carbon, BN_x, or CN_x phases, implying that carbon, carbon nitride, and boron nitride may be in the amorphous form, i.e., as a-(BCNO).

As stated above, we suggested the formation of TiC crystalline phase based on the analysis of an XRD pattern. However, we didn't detected Ti–C bonds by XPS (C1s spectrum). So, we suppose that the XRD peaks, which we associated with TiC phase, originate most likely from TiB phase since these compounds exhibit close XRD lines.

Summarizing the above discussion, we can now propose the structure of Ti–B–C–N films to be a mixture of nc-TiN/nc-TiB_x/nc-TiO_x phases embedded into an amorphous a-C/a–CN/a–BN/a-BC matrix. It should be noted that the existence of TiN amorphous phase was also considered to be feasible based on the Ti–B–N ternary phase diagram [5].

Mechanical properties

Now, with the structural and chemical bond information on the films under study it is reasonable to discuss the hardness measured of the films. There was a clearly observable increase in the hardness of the Ti–B–C–N film prepared with 25% nitrogen in Ar/N_2 gas mixture in comparison with the film deposited in pure Ar atmosphere (Fig. 3). An increase in the film hardness with an addition of nitrogen to a gas mixture can be related apart of TiB_x phase to the formation of the nanocrystalline phases TiN and TiO_x in a film, which exhibit a high hardness. However, further increase of the nitrogen amount in the gas mixture resulted in a noticeable decrease in the film hardness. The formation of an amorphous matrix at high nitrogen content in a work gas mixture is suggested to occur at the expense of a decrease in the percentage of hard TiN and TiB_x phases [5]. So, the amorphous phases, which surround hard nanocrystals, don't favor blocking of these hard phase grains, thereby inducing softening of the film. The decrease in hardness of Ti–B–C–N films deposited by magnetron sputtering of Ti/B_4C target with increase of the N_2/Ar ratio in the working gas mixture was also observed in [8], where the target composed of external ring of titanium and internal rounded disk of B_4C was used.

By scratch testing, a significant increase in adhesive strength of multicomponent Ti–B–C–N films was evidenced in terms of critical load values compared to the film deposited in pure Ar atmosphere (30 cN vs. 7 cN, respectively). Note that increased adhesion strength was a result of an addition of nitrogen to the gas mixture, i.e., even the film deposited with 25% N_2 in gas mixture exhibited the increased adhesion strength, and further addition of nitrogen

in a higher amount had virtually no effect on that parameter. An improvement of the scratch resistance of Ti–B–C–N films could be associated with a decrease in stress gradient between the film and the substrate [22].

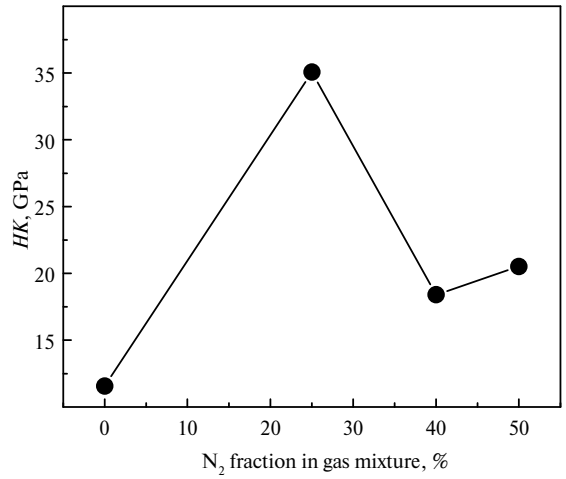

Fig. 3. Knoop hardness of Ni–B–C–N films as a function of a nitrogen fraction in the gas mixture.

Friction is a complicated phenomenon, which is governed by many parameters such as surface roughness, applied load, sliding speed, contact geometry, etc. Generally, the friction performance is evaluated in terms of friction coefficient. The film, which mainly consists of nanocrystalline Ti and TiB phases, deposited in pure Ar atmosphere has the friction coefficient 0.29. With addition of nitrogen to the working gas mixture the friction coefficient of films slightly decreased (0.24 for 25% N_2 in the gas mixture). This can be explained by the fact that amorphous CN has lubricating properties due to its graphite-like structure and low hardness [23]. Amorphous carbon also contributes to lowering hardness of Ti–B–C–N films under study. Further increase in the nitrogen amount in Ar/N_2 gas mixture resulted in some increase in friction coefficient (0.27 for film deposited with 50% N_2 in a gas mixture). As is seen, the friction coefficient changed a little with addition of nitrogen, and this can be the result of low content of amorphous C and CN components in the film structure.

CONCLUSIONS

Hard quaternary Ti–B–C–N films have been deposited onto Si (100) substrates by a dc magnetron sputtering of the bi-component Ti/B_4C target. From XRD and XPS study it could be suggested that the films had composite microstructure consisted of Ti/TiB nanocrystallites solely or of nc-TiN/nc-TiB_x/nc-TiO_x phases embedded into the a-C/a-CN/a-BN/a-BC amorphous matrix. The Knoop hardness exhibited the maximum value 33 GPa for the film deposited with 25% nitrogen content of the working gas mixture. The friction coefficient of films changed little, and with 25% N_2 exhibited the lowest value. The Ti–B–C–N films showed the increased adhesion strength compared with Ti–B–C coatings.

Плівки в четверній Ti–B–C–N системі нанесено на Si (100) підкладки методом магнетронного на постійному струмі розпилення двохкомпонентної Ti/B_4C мішені в суміші газів Ar/N_2 із різною кількістю азоту в суміші (від 0 до 50 %). Плівки досліджували методами рентгенівської дифракції, рентгенівської фотоелектронної спект-

роскопії, індентування та шкрябання. Встановлено, що плівки мають нанокомпозитну структуру, яка складається лише із нанокристалітів (нк) Ti/TiB, якщо осадження проводилося в чистому аргоні, або із нанокристалічних фаз нк-TiN/нк-TiB_x/нк-TiO_x, оточених аморфною a-C/a-CN/a-BN/a-BC матрицею, при осаджені плівок в суміші Ar/N_2. Остання структура є топовою для усіх плівок, незалежно від кількості азоту в газовій суміші. Твердість плівок по Кнупу спочатку збільшувалась при додаванні азоту в газову суміш, досягнувши максимального значення 33 ГПа при 25 % азоту в суміші, а потім зменшувалась. Коефіцієнт тертя плівок змінювався неістотно при додаванні різної кількості азоту в суміш, і при 25 % N_2 виявив найменше значення. Адгезійна міцність Ti–B–C–N-плівок на кремнії виявилася вищою, ніж у Ti–B–C-плівок.

***Ключові слова**: магнетронне розпилення, нанокомпозит, структура, механічні властивості.*

Пленки в четверной системе Ti–B–C–N осаждены на Si (100) подложки методом магнетронного на постоянном токе распыления двухкомпонентной Ti/B_4C мишени в смеси газов Ar/N_2 с разным количеством азота в смеси (от 0 до 50 %). Пленки исследовали методами рентгеновской дифракции, рентгеновской фотоэлектронной спектроскопии, индентирования и царапания. Установлено, что пленки имеют нанокомпозитную структуру, состоящую только из нанокристаллитов (нк) Ti/TiB, если осаждение проводилось в чистом аргоне, или из нанокристаллических фаз нк-TiN/нк-TiB_x/нк-TiO_x, окруженных аморфной a-C/a-CN/a-BN/a-BC матрицей, при осаждении пленок в смеси Ar/N_2. Последняя структура характерна для всех пленок независимо от количества азота в газовой смеси. Твердость пленок по Кнупу сначала возросла при добавлении азота в газовую смесь, достигнув максимального значения 33 ГПа при 25 % азота в смеси, а затем снижалась. Коэффициент трения пленок изменялся незначительно при добавлении разного количества азота в смесь, и при 25 % N_2 показал наименьшее значение. Адгезионная прочность Ti–B–C–N-пленок на кремнии оказалась выше, чем у Ti–B–C-пленок.

***Ключевые слова**: магнетронное распыление, нанокомпозит, структура, механические свойства.*

1. *Pogrebnjak A. D., Shpak A. P., Azarenkov N. A., Beresnev V. M.* Structure and properties of hard and superhard nanocomposite coatings // Phys. Usp. – 2009. – **52**. – P. 29–54.
2. *Musil J.* Hard nanocomposite coatings: Thermal stability, oxidation resistance and toughness // Surf. Coat. Technol. – 2012. – **207**. – P. 50–65.
3. *Pogrebnjak A. D., Beresnev V. M.* Nanocoatings nanosystems nanotechnologies. – N. Y.: Bentham Sci. Publ., 2012. – 155 p.
4. *Chaleix L., Machet J.* Study of the composition and of the mechanical properties of TiBN films obtained by d.c. magnetron sputtering // Surf. Coat. Technol. – 1997. – **91**. – P. 74–82.
5. *López-Cartes C., Martinez-Martinez D., Sánchez-López J. C. et al.* Characterization of nanostructured Ti–B–(N) coatings produced by direct current magnetron sputtering // Thin Solid Films. – 2007. – **515**. – P. 3590–3596.
6. *Laurdsen J., Nedforrs N., Jansson U. et al.* Ti–B–C nanocomposite coatings deposited by magnetron sputtering // Appl. Surf. Sci. – 2012. – **258**. – P. 9907–9912.
7. *Zhong D., Moore J. J., Mishra B. M. et al.* Composition and oxidation resistence of Ti–B–C and Ti–B–C–N coatings deposited by magnetron sputtering // Surf. Coat. Technol. – 2003. – **163**–**164**. – P. 50–56.
8. *Tang G., Ma X., Sun M., Xu S.* Magnetron sputtering deposition Ti–B–C–N films by Ti/B_4C compound target // Ibid. – 2009. – **203**. – P. 1288–1291.
9. *Vyas A., Lu Y. H., Shen Y. G.* Mechanical and tribological properties of multicomponent Ti–B–C–N thin films with varied C contents // Ibid. – 2010. – **204**. – P. 1528–1534.
10. *Chen X., Ma S., Xu K., Chu P. K.* Oxidation behavior of Ti–B–C–N coatings deposited by reactive magnetron sputtering // Vacuum. – 2012. – **86**. – P. 1505–1512.
11. Luo Q. H., Lu Y. H. Microstructure and mechanical properties of reactive magnetron sputtered Ti–B–C–N nanocomposite coatings // Appl. Surf. Sci. – 2011. – **156**. – P. 1021–1026.
12. *Tsai Pi-C., Chen W.-J., Chen J.-H., Chang C.-L.* Deposition and characterization of TiBCN films by cathodic arc plasma evaporation // Thin Solid Films. – 2009 – **517**. – P. 5044–5049.
13. *Holzschuh H.* Chemical-vapor deposition of wear resistant hard coatings in the Ti–B–C–N system: properties and metal-cutting tests // Refract. Met. Hard Mater. – 2002. – **20**. – P. 143–149.

14. *Kim K. H., Ok J. T., Abraham S. et al.* Synthesis and mechanical properties of Ti–B–C–N coatings by a plasma-enhanced chemical vapor deposition // Surf. Coat. Technol. – 2006. – **201**. – P. 4185–4189.
15. *Shimada S., Takahashi M., Tsujino J. et al.* Deposition and wear resistance of Ti–B–C–N coatings on WC–Co cutting tools from alkoxide solutions by thermal plasma CVD // Ibid. – 2007. – **201**. – P. 7194–7200.
16. *X-ray* Powder Diffraction Files.
17. *Tsotos C., Baker M. A., Polychronopoulou K. et al.* Structure and mechanical properties of low temperature msgnetron sputtered nanocrystalline (nc-)Ti(N,C) amorphous diamond0like carbon (a-C:N) coatings // Thin Solid Films. – 2010. – **519**. – P. 24–30.
18. *Strydom I. leR., Hofmann S.* The contribution of characteristic energy losses in the core-level X-ray photoelectron spectroscopy peaks of TiN and (TI, Al)N studied by electron energy loss spectroscopy and X-ray photoelectron spectroscopy // J. Electron Spectrosc. Relat. Phenom. – 1991. – **56**. – P. 85–103.
19. *Avasarala B., Haldar P.* Electrochemical oxidation behavior of titanium nitride based electrocatalysts under PEM fuel cell conditions // Electrochimica Acta. – 2010. – **55**. – P. 9024–9034.
20. *Zhou Z. F., Bello I., Lei M. K. et al.* Synthesis and cgaracterization of boron carbon nitride films by radio frequency magnetron sputtering // Surf. Coat. Technol. – 2000. – **128**–**129**. – P. 334–340.
21. *Benko E., Barr T. L., Hardcastle S. et al.* XPS strudy of the cBN–TiC system // Ceram. Int. – 2001. – **27**. – P. 637–643.
22. *Batista J. C. A., Godoy C., Pintaúde G. et al.* An approachto elucidate the different response of PVD coatings in different tribological tests // Surf. Coat. Technol. – 2003. – **174**–**175**. – P. 891–898.
23. *Vyas A., Li L. K. Y., Zhou Z. F., Shen Y. G*. Carbon nitride based hard multilayer films prepared by closed field unbalanced magnetron sputtering // Surf. Eng. – 2006. – **22**. – P. 15–25.

Frantsevich Institute for Problems of Materials Science
National Academy of Sciences of Ukraine

Received 13.02.14